High-temperature supersolid of ^{4}He in a one-dimensional periodic potential

Raina J. Olsen

Phys. Rev. A **91**, 033602 — Published 2 March 2015

DOI: 10.1103/PhysRevA.91.033602

A high-temperature supersolid of ^{4}He in a one-dimensional periodic potential

Raina J. Olsen*
Materials Science and Technology Division, Oak Ridge National Laboratory, Oak Ridge, TN 37831

The search for robust experimental proof of supersolidity has encountered many complicating factors, such as temperature dependent changes in the mechanical properties of solid ^{4}He which mimic the signature of superfluid flow. As a result, the physical existence and true nature of this unique state of matter are still under debate. Here we consider ^{4}He stabilized by a one-dimensional periodic potential whose lattice spacing is similar to the length scale of the ^{4}He-^{4}He interaction. We use the Bogoliubov transformation to calculate the excitation spectrum, finding that when interactions between nearest or next-nearest neighbors are attractive, there is a finite positive gap in energy between the delocalized ground state and the lowest energy excitations, which is significantly larger than the both the lambda temperature and the melting temperature. Not only does this make the system stable against phase separation of particles and vacancies, but it means that it should be possible to observe a supersolid at a high enough temperature that superfluidity in bulk liquid ^{4}He or changes in the mechanical properties of bulk solid ^{4}He do not obscure it. The properties of experimentally achievable materials which could support this type of supersolid are also discussed.

PACS numbers: 03.75.-b,67.80.bd, 05.30.-d

I. INTRODUCTION

A supersolid is a paradoxical state of matter in which certain positions are more likely to contain a particle than others, just as in a classical solid where the particles occupy fixed sites. But in contrast to a classical solid where each particle is localized at a single site, the particles in a supersolid flow without friction between these sites as they do in a superfluid [1]. Since the concept was first proposed over forty years ago [2–4], the physical existence and true nature of a supersolid has been a matter under debate. The first claim of experimental observation of supersolidity [5] both intensified the debate and increased the interest in studying these systems experimentally.

In general, there are two types of supersolid systems currently being considered, but experimental study of both of these systems present complications which have so far prevented definitive proof for the supersolid state. The first is bulk solid ^{4}He, in which the "solid" in supersolid originates entirely from the ^{4}He-^{4}He van der Waals interaction, which is attractive between particles at adjacent lattice sites. Originally the supersolid state in this system was described as a cloud of delocalized vacancies, which exist even in a perfect crystal [3, 4]. Creation of a localized vacancy increases the potential energy because particles at neighboring sites no longer have an attractive interaction with the removed particle, but delocalizing the vacancy decreases the kinetic energy, thus if the kinetic term dominates then creation of delocalized vacancies will be energetically favorable. But recent theoretical studies have found that delocalized vacancies have a finite energy cost at the melting density [6]. At the same time, torsional oscillator experiments with solid ^{4}He looking for the non-classical rotational inertia (NCRI) of superfluid ^{4}He have found that the fraction of ^{4}He with NCRI has a strong dependence on the density of defects in the crystal [7, 8]. As a result, most people in the field now agree that superfluid flow in solid ^{4}He does not occur in the perfect bulk crystal [9, 10], but occurs only along vacancies which collect near defects [10–12] (though there are some exceptions [13].) Not only does this mean that the fraction of particles participating in superfluid flow is quite small and thus difficult to detect, but experiments have also shown that the defects affect the mechanical properties of the solid in a way which can mimic NCRI [14]. Thus both the physical existence of superfluidity in bulk solid ^{4}He and its accurate theoretical description are still being hotly debated.

The second type of supersolid, formed by cold atoms in optical lattices within an atomic trap [15–19], is simpler to describe but has still not been observed. To see a supersolid in which particles (and thus vacancies) are delocalized over the entire system rather than phase separating, it is necessary to have strong interactions between particles which sit at neighboring sites on the lattice [18]. Strong repulsive interactions between neighbors create a solid-like structure, with only certain lattice points occupied [15–19]. Since optical systems have lattice spacings much larger than the length scale of van der Waals interactions, interactions between neighboring lattice sites are long range and must be induced by some additional mechanism [19–21]. While experimental creation of atomic traps and optical lattices are well-understood, offer significant benefits such as the lack of defects and ability to finely control the system, and have been used to

* olsenrj@ornl.gov,

study Bose-Einstein condensation [22–24] and superfluidity [25], creation of optical systems with strong enough long-range interactions to observe the predicted supersolid has not yet been achieved. Additionally, methods to measure properties of optical systems are quite different than those used with condensed matter systems, and will also need to be developed to detect signatures of supersolidity [20]. But because these systems are predicted to have superfluid flow throughout the entire system, the signature of supersolidity should be much larger, thus easier to reliably detect.

We propose a hybrid system which combines the benefits of each of these systems to overcome many of the current difficulties in obtaining strong experimental proof of supersolidity. Our system is composed of ^{4}He occupying an external periodic potential whose lattice spacing is coherent with the particle-particle interactions. Like bulk solid ^{4}He, the strong interactions necessary to create a supersolid state originate naturally from the ^{4}He-^{4}He van der Waals interaction, but the structure of the supersolid is controlled and stabilized by the external potential, as it is in an optical lattice system. Within a certain range of parameters, we find that the ground state is superfluid and also has crystalline order in its density profile, making it a supersolid. As in an optical supersolid, there is superfluid flow throughout the entire system and thus the fraction of NCRI will be much larger and easier to detect than it is in bulk solid ^{4}He. In addition, we find a large gap in energy between this ground state and the lowest energy density excitations, which is an order of magnitude larger than both the lambda point and melting point of bulk ^{4}He. This means that the signature of NCRI from the supersolid ^{4}He in this system should be observable at high enough temperatures that superfluidity in bulk liquid ^{4}He or changes in the mechanical properties of bulk solid ^{4}He do not obscure it.

In this paper, we consider ^{4}He in an idealized one-dimensional potential, finding that the effect occurs only within two narrow ranges of lattice spacing, corresponding to systems in which there are strong attractive interactions between nearest or next-nearest neighbors. To the best of our knowledge, previous studies of supersolids in optical lattice systems have considered only repulsive interactions between neighbors. The need for strong attractive interactions between neighbors, which originate from short-range van der Waals forces, does add an additional complication to experimental study of this system, since the necessary lattice spacing is too small to be achieved with an optical system; instead an appropriate materials system must be found, and lattice spacing is much more difficult to control in materials. However, we have previously found that a quasi-two dimensional system composed of two close parallel graphene sheets can also provide the necessary environment with attractive interactions between certain next-nearest neighbors [26]. In this system, the graphene lattice spacing is fixed, but the distance between the two sheets is varied to provide the correct spacing between neighbors on different sheets. It is likely that other similar materials systems could also be found, such as nanotubes with controllable diameter [27] and opened ends [28].

II. CALCULATIONS

In this work, we begin with a plane-wave basis set and diagonalize the Hamiltonian using the Bogoliubov transformation (BT) [29]. In Sec. II A we shall review the single mode BT, typically used to calculate the spectrum of excitations in bulk superfluid liquid ^{4}He. In Sec. II B, we will use the multi-mode BT to calculate the excitation spectrum in the presence of an external periodic potential, with the results, showing both superfluidity and long-range crystalline order, presented in Sec. II C. In contrast to the BT used with a plane-wave basis set in the present work, other previous studies of the supersolid state in solid ^{4}He generally begin with a basis set of Wannier functions, which are localized at each lattice site, and use a Bose-Hubbard model (BHM) to diagonalize the Hamiltonian. In Sec. II D we will compare our BT calculations with those of a BHM, showing that excited bands must be included in a BHM to capture the results of the multi-mode BT for this system.

A. Single-Mode Bogoliubov Transformation

We shall briefly review the single-mode BT for a homogeneous system of ^{4}He [30], noting its assumptions and approximations and casting the equations in a matrix form which will be used in the next section with the multi-mode BT. (Note that some of the notation may seem unnecessary in the single-mode case, but will be useful in the multi-mode case.) Then we will use the results of the single-mode BT to discuss the approximate effect of an external potential on the excitation spectrum.

Using a plane wave basis set and assuming that there is no external potential, the Hamiltonian is given by

$$\hat{H} = \sum_k E(k)\hat{a}_k^\dagger \hat{a}_k + \sum_{k,k',q} \frac{V(q)}{2\tilde{V}_l} \hat{a}_{k+q}^\dagger \hat{a}_{k'-q}^\dagger \hat{a}_{k'} \hat{a}_k \qquad (1)$$

where $E(k) = \hbar^2 k^2/2m$ is the kinetic energy, $\tilde{V}_l$ is the volume in l dimensions such that the density is $\rho = N/V^l$ where $N = \sum_k \hat{a}_k^\dagger \hat{a}_k$, and $V(q)$ is the Fourier transform of an effective two-body ^{4}He-^{4}He interaction $V_{eff}(x)$. Typically the effective interaction $V_{eff}(x)$ is equivalent to the real ^{4}He-^{4}He interaction, but with the highly repulsive part at $x \to 0$ set to a finite constant. This screening is an approximation for correlation effects, which we discuss in more detail in the Appendix. Here we use the 3D $V(q)$ proposed by Sunakawa *et al.* [31] to match measurements of excitations in bulk superfluid ^{4}He. This interaction potential is shown in Figure 1(a). It is overall highly repulsive, but is negative at $k \sim 2$ Å^{-1}, corresponding to a wavelength of ~ 3.1 Å and reflecting the fact that the

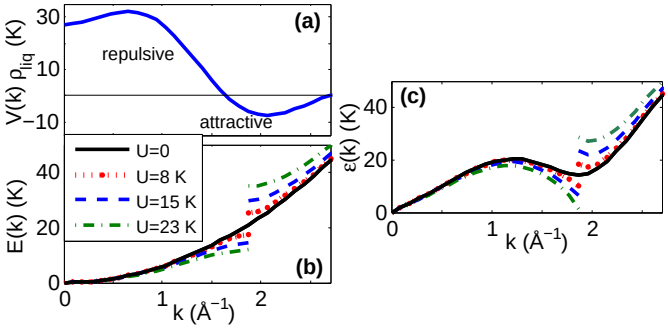

FIG. 1. (Color online) (a) Fourier transform of the ^{4}He-^{4}He interaction energy times the liquid ^{4}He density, ρ_{liq}, in units of Kelvin (K). (b) Single particle energy in a periodic potential $Ucos(Qx)$ with Q=3.75 Å^{-1}. (c) Energy of the elementary excitations calculated by Eq. 12 at ρ_{liq}, using the energies in panel (b).

^{4}He-^{4}He interaction is attractive at these distances. Note that $V(q) = V^*(-q)$, and that the imaginary interaction terms in Eq. 1 always cancel after the sum over q, thus we can take $V(q)$ as real and symmetric.

The BT assumes that the system is at a low enough temperature that the lowest energy state is occupied by a large fraction of the particles, and the number of excitations is small $\sum_{k\neq 0}\hat{a}_k^\dagger\hat{a}_k = \delta N \ll N$. Thus the $k = 0$ state is taken as the trial ground state and because the number of excitations is small, two body interaction terms between two excitations (with $k \neq 0, k' \neq 0$) are neglected. The BT also assumes that because of the macroscopic occupation of the $k = 0$ state, quantum fluctuations of this state may be neglected, and operators for this state are replaced with a c-number,

$$\hat{a}_0^\dagger\hat{a}_0 \equiv N_0 = N - \sum_k \hat{a}_k^\dagger\hat{a}_k \simeq \hat{a}_0\hat{a}_0 \simeq \hat{a}_0^\dagger\hat{a}_0^\dagger \simeq \hat{a}_0\hat{a}_0^\dagger, \quad (2)$$

$$\hat{a}_0^\dagger\hat{a}_0^\dagger\hat{a}_0\hat{a}_0 = N_0^2 \simeq N^2 - 2N\sum_k \hat{a}_k^\dagger\hat{a}_k, \quad (3)$$

Details on derivation of the BT can be found in Pitaevskii and Stringari [30]. Defining $E_0^1 = E(0)$ as the one-body energy of a particle in the lowest energy state, and $E_0^m = \frac{V(0)}{2\tilde{V}_l}$ as the mean field interaction energy between two particles in the system, the Hamiltonian then becomes,

$$\hat{H} = N(E_0^1 + NE_0^m) + \Delta\hat{H} \quad (4)$$

$$\Delta\hat{H} = \sum_{k\neq 0}(E(k) - E(0))\hat{a}_k^\dagger\hat{a}_k \quad (5)$$
$$+N\sum_{k\neq 0}\frac{V(k)}{2\tilde{V}_l}\left[2\hat{a}_k^\dagger\hat{a}_k + \hat{a}_k^\dagger\hat{a}_{-k}^\dagger + \hat{a}_k\hat{a}_{-k}\right].$$

Replacing $2\hat{a}^\dagger\hat{a} = \hat{a}\hat{a}^\dagger + \hat{a}^\dagger\hat{a} - 1 \simeq \hat{a}\hat{a}^\dagger + \hat{a}^\dagger\hat{a}$, and casting $\Delta\hat{H}$ in matrix form,

$$\Delta\hat{H} = \sum_{k\neq 0}[\hat{a}_k^\dagger\hat{a}_{-k}]\begin{bmatrix}\mathcal{E}_k & \lambda_k\\ \lambda_k & \mathcal{E}_k\end{bmatrix}\begin{bmatrix}\hat{a}_k\\ \hat{a}_{-k}^\dagger\end{bmatrix}, \quad (6)$$

$$2\mathcal{E}_k = E(k) - E(0) + \rho V(k), \quad (7)$$

$$2\lambda_k = \rho V(k). \quad (8)$$

Because of the non-zero λ_k terms which mix excitations at k and $-k$, the Hamiltonian is not diagonal in this basis. The Bogoliubov transformation converts to a new diagonal basis where,

$$\Delta\hat{H} = \sum_{k\neq 0}[\hat{b}_k^\dagger\hat{b}_{-k}]\begin{bmatrix}\tilde{\mathcal{E}}_k & 0\\ 0 & \tilde{\mathcal{E}}_k\end{bmatrix}\begin{bmatrix}\hat{b}_k\\ \hat{b}_{-k}^\dagger\end{bmatrix}, \quad (9)$$

through the transformation,

$$\mathbf{M}_k = \begin{bmatrix}u_k & v_k\\ v_k & u_k\end{bmatrix}, \quad (10)$$

$$\begin{bmatrix}\hat{a}_k\\ \hat{a}_{-k}^\dagger\end{bmatrix} = \mathbf{M}_k\begin{bmatrix}\hat{b}_k\\ \hat{b}_{-k}^\dagger\end{bmatrix}. \quad (11)$$

The condition to preserve the boson commutation rules in the new basis, is $u_k^2 - v_k^2 = 1$, with $u_k = cosh(\alpha_k)$, $v_k = sinh(\alpha_k)$, and $tanh(2\alpha_k) = -\lambda_k/\mathcal{E}_k$. This means that for these equations to have a solution, $|\lambda_k| \leq |\mathcal{E}_k|$. When the equations do not have a solution, this indicates that our trial ground state should be discarded.

Note that Eq. 9 diagonalizes the excitations, but does not directly modify the ground state. We will show in Sec II C (begining with Eq. 28) that there is a non-zero number of particles in excited states even at $T = 0$, an effect called quantum depletion which represents an effective modification of the ground state. The quantum depletion at a given k grows as $|\lambda_k| \to |\mathcal{E}_k|$. But recall that in going from Eq. 1 to Eq. 4, the BT makes the assumption that there are few excitations, so that terms which are quadratic in the number of excitations may be neglected. As quantum depletion grows to represent a large fraction of the particles in the system, this assumption becomes inaccurate and thus the BT equations are inaccurate or even insoluble.

Generally speaking, when the BT does not have a solution, this indicates that the ground state should include components at the values of k for which the BT is insoluable. Often this indicates a transition from a Bose-Einstein condensate (BEC) in the delocalized $k = 0$ state to localized states, in which a range of states with small k are occupied. For instance, it is well known that a BEC with attractive interactions is unstable. Under this condition, $\lim_{k\to 0} V(k) < 0$ and Eqs. 7 and 8 show that $|\lambda_k| > |\mathcal{E}_k|$ for small but finite k, thus there is no solution. The BT is not able to explicitly calculate a delocalized to localized transition, but finding no solution for long-wavelength excitations indicates that such a transition will occur.

Scaling the energy so that $E(0) = 0$, the resulting equation for the energy of the excitations is $\epsilon(k) \equiv \tilde{\mathcal{E}}_k$,

$$\epsilon(k) = \sqrt{E(k)^2 + 2E(k)\rho V(k)}. \quad (12)$$

Using the Sunakawa *et al.* [31] potential produces the well-known roton dip in the excitation energy (shown by the unbroken line in Fig. 1(c)), which is caused by using the negative values of $V(k)$ in Eq. 12 at wavelengths ~ 3.1 Å.

As a first approximation, we can estimate the effect of an external periodic potential $Ucos(Qx)$ on the excitation spectrum by using the single particle energy $E(k)$ for the periodic potential, shown in Fig. 1(b) for several values of U. The excitation energies are then calculated by using these values for $E(k)$ in Eq. 12, and are shown in Fig. 1(c).

For the spectra plotted in Figure 1(b)-(c), we have chosen the periodicity of the external potential such that the boundary of the first Brillouin zone at $Q/2$ falls in the roton part of the excitation spectrum. This results in a particularly dramatic change in the excitation spectrum. Even a relatively weak potential opens a large enough band gap at $E(Q/2)$ to significantly reduce the roton energy even further. When $-2\rho V(Q/2)/E(Q/2) > 1$, we find that Eq. 12 no longer has a solution at $Q/2$. As discussed above, this means that our trial ground state, the $k = 0$ state, is not correct, but because the excitations with no solution are not near $k \to 0$, a delocalized to localized transition is probably not the reason. But certainly due to the external potential, states at $\pm Q, \pm 2Q$, ... should also be occupied, and these have not been included in the trial ground state. We should also expect that the trial ground state should include components at $k = \pm Q/2$, since the energy of these excitations has approached zero. In the next section, we will include all of these components using a multi-mode BT.

B. Multi-Mode Bogoliubov Transformation

In the presence of an external potential $Ucos(Qx)$, the Hamiltonian is,

$$\hat{H} = \sum_k \left[E(k)\hat{a}_k^\dagger \hat{a}_k + U/2 \sum_k \hat{a}_k^\dagger \hat{a}_{k\pm Q} \right] \qquad (13)$$

$$+ \sum_{k,k',q} \frac{V(q)}{2\tilde{V}_l} \hat{a}_{k+q}^\dagger \hat{a}_{k'-q}^\dagger \hat{a}_{k'} \hat{a}_k.$$

As in the single mode case, we assume that most of the particles occupy the ground state (g.s.) and that quantum fluctuations of this state can be ignored, but now the ground state will include components at $k \neq 0$ and we will replace each of the operators $\hat{a}_k^\dagger, \hat{a_k}, k \in g.s.$ with c-numbers. We define the ground state as the momentum distribution of the lowest energy many body state, $n_0(k) = \hat{a}_k^\dagger a_k / N_0$, where $N_0 = \sum_{k \in g.s.} \hat{a}_k^\dagger a_k$ is the total number of particles in the ground state. In derivation of Eq. 12, it was assumed that $n_0(0) = 1$. We term any change in this distribution as a deformation of the ground state. Using $\hat{\hat{a}}_0 = \sum_k \sqrt{n_0(k)}\hat{a}_k$, the Hamiltonian for the particles in the ground state is,

$$\hat{H}_0 = E_0^1 \hat{\hat{a}}_0^\dagger \hat{\hat{a}}_0 + E_0^m \hat{\hat{a}}_0^\dagger \hat{\hat{a}}_0^\dagger \hat{\hat{a}}_0 \hat{\hat{a}}_0 + E_0^d \hat{\hat{a}}_0^\dagger \hat{\hat{a}}_0^\dagger \hat{\hat{a}}_0 \hat{\hat{a}}_0, \qquad (14)$$

$$E_0^1 = \sum_k \frac{(\hbar k)^2}{2m} n_0(k) + \frac{U}{2} \sum_k \sqrt{n_0(k \pm Q) n_0(k)}, \qquad (15)$$

$$E_0^m = \frac{V(0)}{2\tilde{V}_l} \sum_{k,k'} n_0(k') n_0(k) = \frac{V(0)}{2\tilde{V}_l}, \qquad (16)$$

$$E_0^d = \sum_{k,k',q \neq 0} \left[\frac{V(q)}{2\tilde{V}_l} \sqrt{n_0(k'+q) n_0(k-q)} \right. \qquad (17)$$

$$\left. \times \sqrt{n_0(k) n_0(k')} \right].$$

The individual terms in these equations were derived from Eq. 13, using $k_1, k_2 \in g.s.$. As in the single-mode case, E_0^1 is the one-body energy of a particle in the ground state, E_0^m is the mean field interaction energy of a particle in the system and is independent of the shape of $n_0(k)$, and we introduce now a new term, E_0^d, which is the interaction energy of a particle which results from the deformation of the ground state. Deformation of the ground state is caused by the presence of the external potential, but also results from the two-body interaction terms whenever the lattice spacing is on the order of the length scale of the interparticle interaction. In fact, we will find that the interesting behavior of this system occurs only when the interactions cause additional deformation of the many-body ground state compared to the single-particle ground state.

We used Eqs. 14-17 to find the ground state for a 1D system using a numerical variational method, starting with $n_0(0) = 1$ and adding components at $n(k)$ which minimize the energy. We found the 1D Fourier transform of the Sunakawa *et al.* [31] pseudo-potential too attractive, resulting in deformation even with $U = 0$ (an unphysical result), thus we estimated $V^{1D}(k) \simeq V^{3D}(k)\rho_{liq}^{2/3}$, with $\rho_{liq} = 0.0218$ Å^{-3} [31].

Figure 2(a)-(b) shows the resultant ground state in real space and momentum space for a choice of $Q = 3.75$ Å^{-1}, for which $V(Q/2) < 0$. As predicted in the previous section, the ground state at high density contains components such that $n_0(Q/2) \neq 0$, leading to $E_0^d < 0$. We note that the single body ground state contains no components at $Q/2$, so this deformation at $Q/2$ is entirely the effect of interactions. By looking at the real space representation of the ground state in Fig. 2(a), we can gain a better physical understanding of this effect. At a density $\rho \to 0$, where interactions are negligible, there are peaks in the probability density a distance 1.67 Å$= 2\pi/Q$ apart, corresponding to each lattice site. But the ^{4}He-^{4}He interaction is highly repulsive at this distance, thus at high density the ground state is deformed so that only every other lattice site is occupied. The fact that $E_0^d < 0$ reflects the fact that the ^{4}He-^{4}He interaction is attractive for next-nearest neighbors on the lattice at a distance of $2 \times 1.67 = 3.35$ Å.

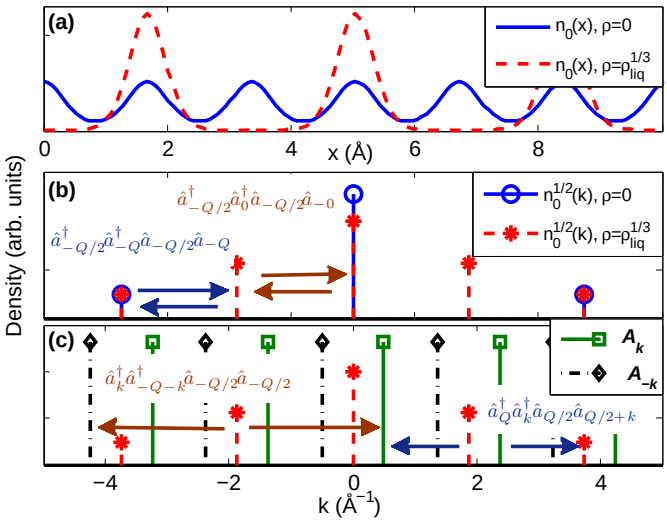

FIG. 2. (Color online) Density in (a) real space and (b) momentum space of the ground state, for Q=3.75 Å^{-1} at average densities of $\rho = 0, \rho_{liq}^{1/3}$. Panel (b) also depicts some of the negative two-body interaction terms in the ground state Hamiltonian which make addition of components at $n_0(Q/2)$ energetically favorable, depicted by arrows that go from the annihilated state to the created state. (c) Density in momentum space of the ground state, and the vectors of excitations which interfere through the ground state. Some of the off-diagonal terms in the Hamiltonian are also depicted by arrows between the annihilated states and created states.

The approximate Hamiltonian for the single-mode case (Eq. 4) contains several off-diagonal terms in which excitations at $\pm k$ interfere through interaction with the ground, $k = 0$ state, such as $\hat{a}_k^\dagger \hat{a}_{-k}^\dagger \hat{a}_0 \hat{a}_0 \sim N \hat{a}_k^\dagger \hat{a}_{-k}^\dagger$, and the single-mode BT transforms to a new basis in which these off-diagonal terms cancel. But because the deformed ground state contains more components, we should expect more off-diagonal terms. As with the single mode case, we will use an approximate Hamiltonian which includes the single-particle energy of the excitations and the interaction energy between a particle in the ground state and an excitation, but the interaction between two excitations will neglected.

$$\hat{H} = \hat{H}_0 + \sum_{k \notin g.s.} \left[\frac{\hbar^2 k^2}{2m} \hat{a}_k^\dagger \hat{a}_k + \frac{U}{2} \hat{a}_k^\dagger \hat{a}_{k \pm Q} \right] \tag{18}$$
$$+ \sum_{k_0 \in g.s., k \notin g.s.} \frac{V(0)}{2V_l} 2\hat{a}_{k_0}^\dagger \hat{a}_k^\dagger \hat{a}_k \hat{a}_{k_0}$$
$$+ \sum_{k_0, k_0' \in g.s., k \notin g.s.} \frac{V(k)}{2V_l} \left[2\hat{a}_{k_0+k}^\dagger \hat{a}_{k_0'}^\dagger \hat{a}_{k_0'+k} \hat{a}_{k_0} \right.$$
$$\left. + \hat{a}_{k_0}^\dagger \hat{a}_{k_0'}^\dagger \hat{a}_{k_0'+k} \hat{a}_{k_0-k} + \hat{a}_{k_0+k}^\dagger \hat{a}_{k_0'-k}^\dagger \hat{a}_{k_0'} \hat{a}_{k_0} \right],$$

where the last two terms are off-diagonal. There are indeed many more of these off-diagonal elements in this Hamiltonian, such as $\hat{a}_k^\dagger \hat{a}_{Q-k}^\dagger \hat{a}_Q \hat{a}_0$ (using $k_0 = 0, k_0' = Q$ in the last term). This means that an excitation at k interferes with other excitations at many wavevectors besides just $-k$, necessitating a multi-mode BT.

Inserting $\hat{\tilde{a}}_0^\dagger \hat{\tilde{a}}_0 = N_0$ and Eqs. 2 and 3 into Eq. 14, and the result into Eq. 18, we obtain

$$\hat{H} = N(E_0^1 + NE_0^m + NE_0^d) + \Delta\hat{H} \tag{19}$$
$$\Delta\hat{H} = \sum_{k \notin g.s.} \left[\left(\frac{\hbar^2 k^2}{2m} - E_0^1 - 2NE_0^d \right) \hat{a}_k^\dagger \hat{a}_k + \right. \tag{20}$$
$$\left. \frac{Q}{2} \hat{a}_k^\dagger \hat{a}_{k \pm Q} \right] + \sum_{k_0, k_0' \in g.s., k \notin g.s.} \frac{V(k)N}{2V_l} \sqrt{n_0(k_0) n_0(k_0')} \times$$
$$\left[2\hat{a}_{k_0+k}^\dagger \hat{a}_{k_0'+k} + \hat{a}_{k_0'+k} \hat{a}_{k_0-k} + \hat{a}_{k_0+k}^\dagger \hat{a}_{k_0'-k}^\dagger \right].$$

The off-diagonal terms may be expressed in matrix form using vectors of creation and annihilation operators. We define $K = (k | n_0(k) \neq 0)$, $K_l < K_{l+1}$ as the discrete ordered set of $m+1$ wavevectors contained in the ground state, and assume that the ground state is symmetric about $k = 0$ such that $K_l = -K_{m-l}$. We also define $\hat{\mathbf{A}}_k = [\hat{a}_{K_0+k} \ldots \hat{a}_{K_m+k}]$ and $\hat{\mathbf{A}}_{-k} = [\hat{a}_{K_m-k} \ldots \hat{a}_{K_0-k}]$ as vectors of annihilation operators, with $\hat{\mathbf{A}}_k^\dagger$ and $\hat{\mathbf{A}}_{-k}^\dagger$ the corresponding vectors of creation operators. Figure 2(c) depicts these vectors. Again using $2\hat{a}^\dagger \hat{a} \simeq \hat{a}\hat{a}^\dagger + \hat{a}^\dagger \hat{a}$, and $k_0 = K_l$ with k_0' set by K_l, K_i, K_j, and the condition of momentum conservation, we obtain ΔH in matrix form,

$$\Delta\hat{H} = \frac{1}{m+1} \sum_{k \notin g.s.} [\hat{\mathbf{A}}_k^\dagger \hat{\mathbf{A}}_{-k}] \begin{bmatrix} \boldsymbol{\mathcal{E}}_k & \boldsymbol{\lambda}_k \\ \boldsymbol{\lambda}_k & \boldsymbol{\mathcal{E}}_k \end{bmatrix} \begin{bmatrix} \hat{\mathbf{A}}_k \\ \hat{\mathbf{A}}_{-k}^\dagger \end{bmatrix}, \tag{21}$$
$$2\mathcal{E}_{k,ij} = \left(\frac{\hbar^2 (K_i + k)^2}{2m} - E_0^1 - 2NE_0^d \right) \delta_{ij} + \tag{22}$$
$$\frac{U}{2} \delta_{K_i \pm Q, K_j} + \rho \sum_{l=[0,m]} \left[V(K_i - K_l + k) \times \right.$$
$$\left. \sqrt{n_0(K_l) n_0(K_j - K_i + K_l)} \right],$$
$$2\lambda_{k,ij} = \rho \sum_{l=[0,m]} \left[V(K_i - K_l + k) \times \right. \tag{23}$$
$$\left. \sqrt{n_0(K_l) n_0(K_i + K_{m-j} - K_l)} \right].$$

where the term $1/(m+1)$ in front of Eq. 21 accounts for multiple instances of $k' = k + K_l$ over the $m+1$ values of K_l. The real multi-mode BT converts to a new basis, $\hat{\mathbf{B}}$,

$$\Delta\hat{H} = \frac{1}{m+1} \sum_k [\hat{\mathbf{B}}_k^\dagger \hat{\mathbf{B}}_{-k}] \begin{bmatrix} \tilde{\boldsymbol{\mathcal{E}}}_{\boldsymbol{k}} & \mathbf{0} \\ \mathbf{0} & \tilde{\boldsymbol{\mathcal{E}}}_{\boldsymbol{k}} \end{bmatrix} \begin{bmatrix} \hat{\mathbf{B}}_k \\ \hat{\mathbf{B}}_{-k}^\dagger \end{bmatrix}, \tag{24}$$

where $\tilde{\boldsymbol{\mathcal{E}}}_{\boldsymbol{k}}$ is diagonal, $\tilde{\boldsymbol{\lambda}}_{\boldsymbol{k}} = \mathbf{0}$, $\epsilon(K_i + k) = \tilde{\mathcal{E}}_{k,ii}$, and

$$\mathbf{M}_k = \begin{bmatrix} \mathbf{u}_k & \mathbf{v}_k \\ \mathbf{v}_k^\dagger & \mathbf{u}_k^\dagger \end{bmatrix}, \tag{25}$$

$$\begin{bmatrix} \hat{\mathbf{A}}_k \\ \hat{\mathbf{A}}_{-k}^\dagger \end{bmatrix} = \mathbf{M}_k \begin{bmatrix} \hat{\mathbf{B}}_k \\ \hat{\mathbf{B}}_{-k}^\dagger \end{bmatrix}, \tag{26}$$

Many properties of this transformation have been discussed in other work [32–35] which we will not repeat here. However, we note that the condition for the commutation rules to be preserved in the new basis is,

$$\mathbf{M}^\dagger \begin{bmatrix} \mathbb{1} & \mathbf{0} \\ \mathbf{0} & -\mathbb{1} \end{bmatrix} \mathbf{M} = \begin{bmatrix} \mathbb{1} & \mathbf{0} \\ \mathbf{0} & -\mathbb{1} \end{bmatrix}, \tag{27}$$

which reduces to the familiar $u^2 - v^2 = 1$ in the single mode case. Clearly if $\mathbf{M}$ and $\mathbf{M}_r$ both meet this condition, so does $\mathbf{M}\mathbf{M}_r$. Thus we solved for $\mathbf{M}$ using an iterative Monte Carlo method: starting with $\mathbf{M}_0 = \mathbb{1}$, repeatedly generating a random matrix $\mathbf{M}_r$ for which Eq. 27 is true, and setting $\mathbf{M}_{i+1} = \mathbf{M}_i\mathbf{M}_r$ if the off-diagonal elements of the Hamiltonian are smaller in the new basis.

C. Results

In two cases, we find a solution for $\mathbf{M}$ ($\tilde{\boldsymbol{\mathcal{E}}}_{\boldsymbol{k}}$ diagonal and $\tilde{\boldsymbol{\lambda}}_{\boldsymbol{k}} = \mathbf{0}$) where there is a positive gap in energy between the ground state n_0 and the lowest energy Bogoliubov excitation. Figure 3(a)-(b) shows the gap size as a function of Q, ρ, and a dimensionless parameter c describing the potential strength $U = -(c\hbar Q)^2/2m$. In general, an energy gap appears at high density in a periodic potential where either Q or $Q/2$ falls into the roton region, referred to as "Case 1" and "Case 2" respectively. Figure 3(c)-(d) shows representative excitation spectra for each case.

In every case where a positive energy gap appears, $E_0^d < 0$. Mathematically, this can be understood by examining Eq. 22, which shows that the diagonal of $\boldsymbol{\mathcal{E}}_k$ is offset by $-NE_0^d$. As discussed in the single-mode case, we require $|\lambda_k| \leq |\mathcal{E}_k|$ for the equations to have a solution. For the multi-mode transformation, the condition is that $|\tilde{\lambda}_{k,ii}| \leq |\tilde{\mathcal{E}}_{k,ii}|$ in a basis where both $\tilde{\boldsymbol{\mathcal{E}}}_k$ and $\tilde{\boldsymbol{\lambda}}_k$ are diagonal. For $E_0^d = 0$, we find $\lim_{k\to 0} |\tilde{\lambda}_{k,ii}| = |\tilde{\mathcal{E}}_{k,ii}|$ and $\lim_{k\to 0} |v_k, ii| = |u_k, ii| = \infty$, which leads to $\lim_{k\to 0} \epsilon(k) = 0$. Meanwhile, if E_0^d is negative, we find $\lim_{k\to 0} |\tilde{\lambda}_{k,ii}| < |\tilde{\mathcal{E}}_{k,ii}|$, but they are never equal, and it can be shown that this means $|v_k|$ and $|u_k|$ never approach infinity and $\epsilon(k)$ never approaches zero.

Physically, we can understand this by comparing the present system to the corresponding classical case of ^{4}He adsorbed on graphene, where the ground state describes a solid commensurate (aligned) with the underlying periodic potential. As the wavelength of the phonons approaches infinity ($k \to 0$), the phonons represent vibration of the entire system back and forth together, resulting in no net change to the interparticle interactions, but moving the particles out of the minima in the potential

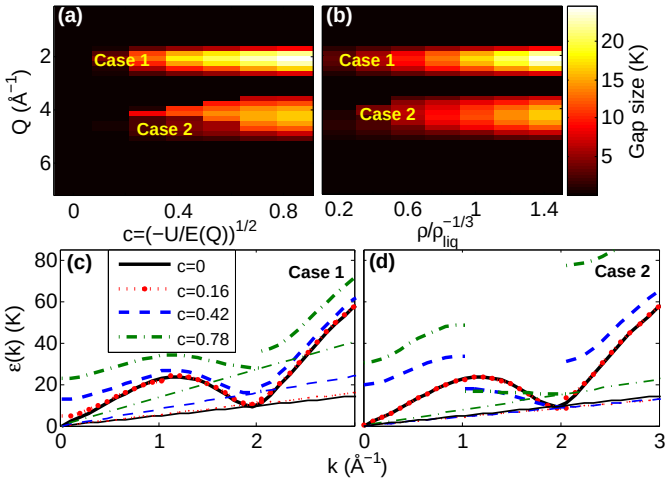

FIG. 3. (Color online) Energy gap between the ground superfluid state and lowest energy excitation for (a) $\rho = 1.4\rho_{liq}^{1/3}$ and (b) $c = 0.92$. Excitation spectrum $\tilde{\mathcal{E}}(k)$ at $\rho = 1.2\rho_{liq}^{1/3}$ for (c) $Q = 2.06$ Å^{-1} and (d) $Q = 4.11$ Å^{-1} with several values of c. Panels (c) and (d) also show $v_c\hbar k$ for each excitation spectrum, where v_c is the critical velocity.

and thus coming at a finite energy cost in the presence of a lattice potential [37]. This finite gap between the ground state and the longest wavelength phonons has been measured by neutron scattering [38]. The gap in the excitation spectrum increases the stability of the solid phase and thus raises the melting temperature. Here, we observe a similar behavior, with the presence of the external potential breaking translational symmetry [36] and creating a finite gap between the excitation spectrum and the ground state, except here the ground state is superfluid.

$E_0^d < 0$ with Q or $Q/2$ falling into the roton region corresponds to there being strongly attractive interactions between either nearest or next-nearest neighbors respectively, corresponding to lattice spacings of ∼3.1 Å and ∼1.5 Å respectively. We note that the lattice spacing in graphene is 2.46 Å, which falls outside of both "Case 1" and "Case 2". At intermediate values of Q which do not fall into either of these cases, we could not find a solution for the multi-mode BT. Instead, we find that we reach a solution in which $\tilde{\boldsymbol{\mathcal{E}}}_{\boldsymbol{k}}$ and $\tilde{\boldsymbol{\lambda}}_{\boldsymbol{k}}$ are diagonal, but $|\tilde{\lambda}_{k,ii}| > |\tilde{\mathcal{E}}_{k,ii}|$ for some small values of k. As mentioned previously, finding no solution at small values of k indicates that the delocalized trial ground state n_0 should be discarded, and that the real ground state likely consists of particles in localized states, which is consistent with the experimental results for ^{4}He on graphene. In Figure 3, we report an energy gap of zero in these cases where we find no solution because we believe that a BHM is better at distinguishing between an insulating state and a gapless superfluid state. We will discuss the BHM in the context of this problem in the next section.

At chemical potential μ and temperature T, since the

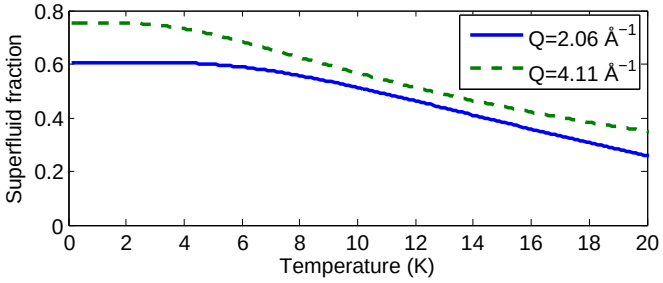

FIG. 4. (Color online) Superfluid fraction as a function of temperature for $\rho = 1.2\rho_{liq}^{1/3}$ and $Q = 2.06$ Å^{-1} ("Case 1") and $Q = 4.11$ Å^{-1} ("Case 2").

quasi-particle excitations are bosons, their average occupation is

$$< \hat{b}_k^\dagger \hat{b}_k >= \frac{1}{e^{(\epsilon(k)-\mu)/k_B T} - 1}, \tag{28}$$

where k_B is the Boltzmann constant. But the average number of real particles in excited states must be calculated from the average numbers of excitations using the BT, giving

$$< \hat{a}_k^\dagger \hat{a}_k > = \sum_j \Big[u^*_{k,jm/2} u_{k,jm/2} < \hat{b}^\dagger_{K_j+k} \hat{b}_{K_j+k} > + v^*_{k,jm/2} v_{k,jm/2} < \hat{b}_{-K_j-k} \hat{b}^\dagger_{-K_j-k} > \Big], \tag{29}$$

where we have used the symmetry of the ground state, $K_{m/2} + k = k$, in the matrix multiplication. Using $< \hat{b}_{-K_j-k} \hat{b}^\dagger_{-K_j-k} >=< \hat{b}^\dagger_{K_j+k} \hat{b}_{K_j+k} > +1$, we obtain,

$$< \hat{a}_k^\dagger \hat{a}_k >= \sum_j \left[\frac{|u_{k,jm/2}|^2 + |v_{k,jm/2}|^2}{e^{(\epsilon(K_j+k)-\mu)/k_B T} - 1} + |v_{k,jm/2}|^2 \right] \tag{30}$$

The second term in Eq. 30 is temperature independent, and is known as the quantum depletion. It is described as the effect of the strong interactions which tend to push particles out of the ground state even at $T = 0$. The resultant increase in kinetic energy represents the zero-point energy of the relative motion between the interacting particles. The first term in Eq. 30 is temperature dependent, and is known as the thermal depletion.

In bulk liquid ^{4}He, the quantum depletion at $T = 0$ is quite large, ∼91% [39]. We find that there is significantly less quantum depletion in our system: 39.3% in "Case 1" and 24.6% in "Case 2" (with $c = 0.92$, $\rho = 1.2\rho_{liq}^{1/3}$, and $Q = 2.06, 4.11$ Å^{-1} respectively.) This is because interactions strongly deform the density of the ground state instead, and the quantum depletion is relatively small. Mathematically, this can be directly related to the presence of a gap. The gap appears because $|v_{k,jm/2}|$ never approaches infinity, and this also reduces the magnitude of the quantum depletion.

In Figure 4, we show the fraction of particles in the ground state, defined as N_0/N, where,

$$N_0 = N - \sum_{k \neq 0} < \hat{a}_k^\dagger \hat{a}_k > . \tag{31}$$

We have used the μ of an equivalent non-interacting 1D boson gas at N, T in Eq. 30 to calculate the average number of particles in excited states. Figure 4 shows that N_0/N remains fixed at 60-75% up to T =2–4 K (depending on parameters), and then drops off slowly. Both the flat region and the slow fall-off are directly related to the presence of the gap in the excitation spectrum, which reduces the thermal depletion of the ground state. Because the ground state has diagonal long-range order, and describes a delocalized state in which particles/vacancies are spread out over the entire system, we call this state a supersolid and N_0/N the superfluid fraction.

In contrast, for a 3D bulk superfluid, $\mu = 0$ is used instead, which assumes that the N_0 particles form a Bose-Einstein condensate in the ground state. But the Mermin-Wagner-Hohenberg theorem states that there cannot be off-diagonal long-range order (ODLRO) in less than three dimensions. This is a general theorem; Hohenberg [40] applied it to fluctuations in Bose liquids, showing that there can be no ODLRO and thus no BEC in any 1D or 2D system. Similar theorems also prevent diagonal long-range order in less than three dimensions for systems with continuous translational symmetry, but the underlying periodic potential breaks translational symmetry [36], permitting long-range crystalline order in this system (just as it permits a classical 2D solid for ^{4}He adsorbed on graphite [37, 38]). However, presence of a periodic external potential does not permit ODLRO.

Thus the superfluid fraction is in the ground density state, but the phase may still fluctuate. The wavefunction of all N_0 particles is thus,

$$\psi = \sqrt{n_0(x)} e^{i\phi(x)}. \tag{32}$$

Note that this wavefunction has an irrotational velocity field, just as in a bulk 2D or 3D superfluid. However, it is likely that phase excitations no longer take the form of simple vortices, with $\phi(r, \theta) = m\theta$, where m is any integer. This is for two reasons. First, vortices are solutions of the Gross-Pitaevskii equation, which assumes the particle-particle interaction can be approximated by a delta-function interaction, while the behavior we have predicted in the present work emerges only with a finite-width interaction. Secondly, since $n_0(x)$ is not equal to a constant, the Gross-Pitaevskii Hamiltonian may generate interference terms $\nabla\sqrt{n_0(x)} \cdot \nabla e^{i\phi(x)}$.

While a treatment of the Berezinsky-Kosterlitz-Thouless transition (which originates from the behavior of phase excitations) in this system is beyond the scope of this work, we do note that phase excitations of the form $e^{im\theta}$ will not have diverging velocities in their core if their centers are at the minima in $n_0(x)$. To prevent diverging energy for vortices in normal bulk systems, the density of

the superfluid is normally multiplied by a function that goes to zero at the core center. In this system, that function should vary as a function of x, and thus should lead to significantly different dynamics for the phase excitations in the present system compared to bulk systems.

D. Comparison With Other Models

Here we have used a plane-wave basis set and diagonalized the Hamiltonian using the BT [29]. In contrast, most previous studies of the supersolid state have used an extended Bose-Hubbard Hamiltonian, with a basis of Wannier functions ψ_i localized at each lattice site i. A simple hard-core Bose-Hubbard Hamiltonian is,

$$\hat{H} = \sum_i \Big[-t(\hat{c}_i^\dagger \hat{c}_{i+1} + H.c.) - \mu \hat{c}_i^\dagger \hat{c}_i + V \hat{c}_i^\dagger \hat{c}_{i+1}^\dagger \hat{c}_{i+1} \hat{c}_i \Big] \tag{33}$$

where $\hat{c}_i^\dagger$ creates a particle in the lowest energy band at site i and permits only one particle per site, μ is the chemical potential, V is the interaction energy between particles at neighboring sites on the lattice, and $-t$ is a negative value representing the decrease in kinetic energy when particles hop between sites. BH models similar to these have been thoroughly explored for positive (repulsive) V [15–18, 20]. But of course in a system of ^{4}He with a small lattice spacing, V is attractive (negative), and delocalizing particles throughout the entire system involves a trade-off between potential and kinetic energy, which we can understand by considering a simple example.

Figure 5(a) depicts a solid many-body state consisting of N particles on N sites, which has an energy of NV. If a vacancy is created inside the solid, as shown in Fig. 5(b), the energy will be $(N-2)V - 2t$, a change of $-2V - 2t$. (Note that the diagonalized state will be a normalized linear combination of states with the vacancy at different positions, $(|011\cdots> + |101\cdots> + |110\cdots> + \ldots)/\sqrt{N}$, each of which have the same energy.) Because V is negative, removing a particle increases the potential energy by $-2V$. But if particles jump into this vacancy from neighboring sites, their kinetic energy decreases by $-2t$. If the total is positive, then the solid is the ground state, and if the total is negative, then creation of delocalized vacancies inside the solid is energetically preferred and the ground state is a superfluid. Theoretical work with bulk solid ^{4}He at the melting density, 0.0287 Å^{-3}, finds that the potential energy term dominates and thus the ground state is solid $n_0(x)$. To make a superfluid the ground state, the kinetic term must dominate instead. We will show that the kinetic term becomes more important in the system presented in this work because particles are pushed into higher-order bands by interactions.

Inclusion of higher-order bands leads to more complex behavior due to the larger amount of overlap between excited Wannier functions at neighboring lattice sites

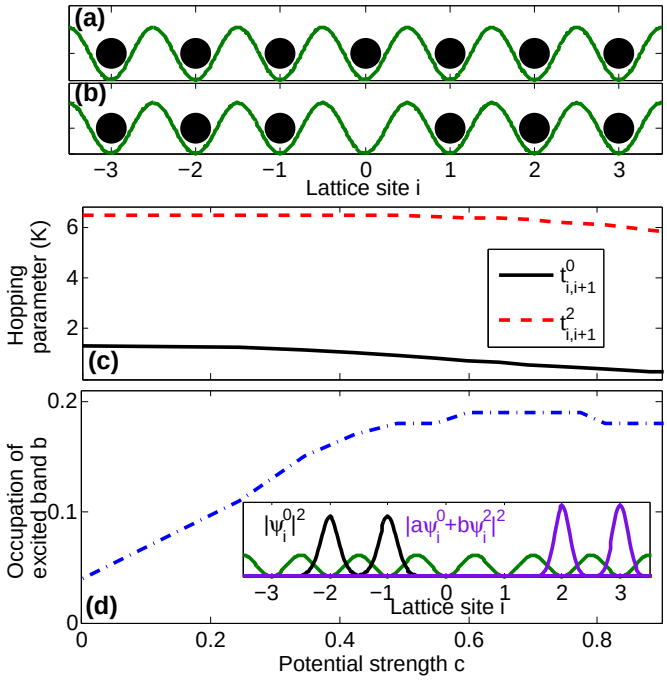

FIG. 5. (Color online) Bose-Hubbard model for an external potential $-Ucos(Qx)$ with $Q = 2.06$ Å^{-1}, corresponding to a lattice spacing of $a = 3.05$ Å, and varying $U = -(c\hbar Q)^2/2m$. (a) An insulating solid state with one particle at each site. (b) State with a vacancy inside the solid, which can hop to different positions. (c) Value of the hopping parameter between two adjacent sites for particles in the lowest energy band and second excited band, $\alpha = 0, 2$. (d) Occupation of the second excited band for a solid state which minimizes the energy. Inset shows wavefunctions at adjacent sites for $c = 0.89$ for the $\alpha = 0$ states (left), and for the lowest energy combination of the $\alpha = 0, 2$ states (right).

[19]. Based on the results of the BT, which found that the interactions resulted in additional deformation of the ground state beyond the deformation caused by the external potential, we should expect that the interactions should push particles into excited bands in a BHM. A BH Hamiltonian with excited bands which can capture the behavior of the present system is,

$$\hat{H} = \sum_{i,\alpha} \Big[-t_\alpha (\hat{c}_{i,\alpha}^\dagger \hat{c}_{i+1,\alpha} + H.c.) + (E_\alpha - \mu) \hat{c}_{i,\alpha}^\dagger \hat{c}_{i,\alpha} \Big] + \sum_{i,\alpha_1,\alpha_2,\alpha_3,\alpha_4} \Big[2V_{i,i+1,i+1,i}^{\alpha_1,\alpha_2,\alpha_3,\alpha_4} \hat{c}_{i,\alpha_1}^\dagger \hat{c}_{i+1,\alpha_2}^\dagger \hat{c}_{i+1,\alpha_3} \hat{c}_{i,\alpha_4} + 2V_{i,i+1,i,i+1}^{\alpha_1,\alpha_2,\alpha_3,\alpha_4} \hat{c}_{i,\alpha_1}^\dagger \hat{c}_{i+1,\alpha_2}^\dagger \hat{c}_{i,\alpha_3} \hat{c}_{i+1,\alpha_4} \Big] \tag{34}$$

where α labels the band and E_α is the band energy. Note that because the interaction has a finite width on the order of the lattice spacing ($d = 2\pi/Q$), both direct and exchange interactions are important and included in Eq.

34, with matrix elements given by,

$$V^{\alpha_1,\alpha_2,\alpha_3,\alpha_4}_{i_1,i_2,i_3,i_4} = \frac{1}{2}\int \psi^*_{i_1,\alpha_1}(x_1)\psi^*_{i_2,\alpha_2}(x_2)V(x_1-x_2) \times\psi_{i_3,\alpha_3}(x_2)\psi_{i_4,\alpha_4}(x_1)dx_1dx_2. \quad (35)$$

Figure 5(c) shows that the energy of the hopping term for the second excited band is much larger than for the lowest energy band. This means that the kinetic term becomes more important when excited bands are occupied.

To test our hypothesis that interactions push particles into excited bands, we calculated the energy of the solid state $\Pi_i(a\psi_{i,0} + b\psi_{i,2})$ as a function of b, with $a^2 + b^2 = 1$ using the Dupont-Roc *et al.* [41] pseudo-potential for $V(x)$. Figure 5(d) shows the value of b for which the energy is minimized as a function of potential strength. We do find that interactions push particles into higher bands, and this becomes more significant as the potential strength increases. The minimized wavefunction (shown in the inset of Fig 5(d)) tends to localize the particles more strongly at lattice points than the lowest band Wannier function because $V(d)$ is attractive, while $V(x < d/2)$ is repulsive. But when the potential strength is quite weak, $\psi_{i,2}$ is not localized by the periodic potential, and so the interaction energy is not minimized by occupation of this band. As the potential gets even stronger, we would expect other bands $\psi_{i,4}, \psi_{i,6}\ldots$ to also become important.

In principle, this BHM model could be solved, though it is much more complex. But to accurately use the model to predict properties of a potential experimental system, we must use an accurate pseudo-potential. Here we have used the $V(x)$ of Dupont-Roc *et al.* [41], which has an arbitrarily chosen shape for the soft core whose parameters were set to match three experimental parameters - the density, energy, and compressibility of bulk liquid ^{4}He. In contrast, the $V(k)$ used in the BT calculations was chosen to match measurements of $\epsilon(k)$ in bulk superfluid ^{4}He, which provide an accurate estimation of $V(k)$ over a broad range of k. Because phase information on $V(k)$ is not measured, an accurate representation of $V(x)$ to use in the BHM cannot be extracted directly from $V(k)$.

However, comparison of the BT and the BHM allows us to more easily understand the physical reason for the unique behavior we predict in this system. The presence of the external potential allows particles at adjacent sites to avoid each other's repulsive cores by occupying wavefunctions that are more strongly localized at each lattice site, but which also have higher kinetic energy. Delocalizing the particles by spreading them over multiple sites thus results in a larger reduction in kinetic energy, which is able to overcome the increase in potential energy that comes from creating vacancies inside the solid.

III. DISCUSSION

Here we have shown that when ^{4}He occupies a periodic potential with a lattice spacing similar to the length scale of the ^{4}He-^{4}He interaction, the lowest energy state describes a system with long-range crystalline order in which particles are delocalized over all the lattice sites, both of which are properties of a supersolid. Generally, a supersolid is concisely described as a system with both diagonal long-range order (in the density) and off-diagonal long range order (in the phase). We will now discuss the precise definition of the supersolid state, arguing that the present system should indeed be considered a supersolid.

Boninsegni and Prokofev [10] say that for a system to be considered a supersolid, the long range crystalline order must occur "spontaneously, exclusively as a result of interactions among elementary constituents." Presumably, this condition is to exclude systems in which a density modulation is imposed by an external potential that would not otherwise exist. However, we argue that the word "exclusively" should be removed from this definition. In the present system, a density modulation is certainly imposed by an external potential, but the predicted behavior occurs *only* when the imposed modulation has the same periodicity as is spontaneously adopted in bulk solid ^{4}He, and the density profile is also perturbed by the interactions to be different than the single-particle state of the same potential. Presence of the external potential simply allows the long range crystalline order to exist in less than three dimensions, and at higher temperatures than normally observed.

While we have shown that the ground state has a significant fraction of particles delocalized over the entire system (rather than confined to a single site), the generally accepted condition for superfluidity is that off-diagonal long-range order in the phase must decay algebraically as a function of distance, rather than exponentially as it does in a classical gas. Popov [42] showed through consideration of phase fluctuations that a homogeneous 2D system at $T = 0$ has off-diagonal long-range order which decays algebraically, whereas a homogeneous 1D system has exponentially decaying ODLRO. (In 3D, there is no decay.) Clearly if there is no superfluidity at $T = 0$, it will not exist at $T > 0$ either. However, simulations have found superfluid flow in certain quasi-1D systems [12] and we also predict superfluid behavior in this 1D system. Because of the complexity of phase excitations in this system, which we discussed in Sec. II C, we have not calculated the off-diagonal order parameter for this system. However, we do note that superfluidity emerges here *only* because of the novel gap in energy we have found between the ground state and excitations in this system. If there were no gap, the number of excitations calculated from Eq. 30 (with the sum properly converted to a Bose integral with a constant density of states near $k \to 0$) would have an infrared divergence even at $T = 0$, thus there would be zero particles left in the delocalized superfluid ground state.

We find the physical reason for using algebraic decay of ODLRO as a condition for superfluidity to be inadaquate. Algebraic decay of long range order indicates that the system is approaching a critical point, which in this case

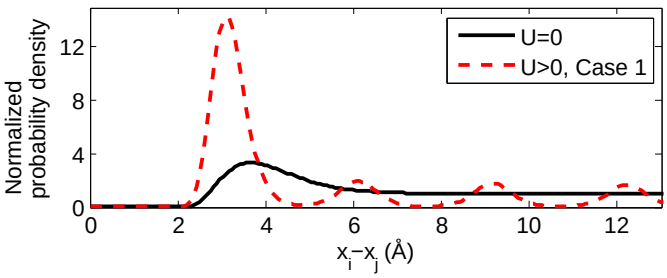

FIG. 6. (Color online) Average correlation between two particles in one dimension at T=2 K, with and without an external potential. The latter case falls under "Case 1", with $c = 0.92$, $\rho = 1.2\rho_{liq}^{1/3}$, and $Q = 2.06$ Å^{-1}.

represents formation of a BEC. But a BEC and a superfluid are not equivalent. For instance, non-interacting BECs are not superfluid, and a bulk 2D superfluid is not a BEC.

Presence of slowly-decaying ODLRO means that at any given instant the phases of the equilibrium wavefunction at two points which are far apart are correlated with one another. Since velocity is the derivative of phase, this means that the velocities of two particles in the superfluid which are not in direct contact with one another are also correlated at any given instant. But many of the unique properties of a superfluid which make it of interest to specialists and novices alike, such as the fountain effect or the tendency of the superfluid to reach the lowest available level in a gravitation field even when it must climb over high barriers to do so, are particular to its time-dependent response to changing conditions in the environment rather than its equilibrium state at a single moment. In a typical bulk system, correlation functions of the many-body state at a time interval $\tau = t_2 - t_1 = 0$ may be able to accurately predict the response of the system to fluctuations over short time intervals, $\tau \simeq 0$. But both the BT and the BHM work in a Fock space, where the many-body state is a product of single-particle states and explicit correlation terms are neglected, except in an approximate way through the choice of the short-range pseudo-potential. But when particle-particle correlations are long-range, the evolution of the system in response to fluctuations can not be accurately predicted by correlation functions at $\tau = 0$.

To investigate particle-particle correlations in this system, we explicitly calculated two-body terms using a mean field method described in detail in the Appendix. Figure 6 shows the resultant correlation probability $\rho_{12}(x_1 - x_2)$, defined as the mean probability density for two-body terms of the many-body quantum state. When there is no external potential, the correlation probability goes to a constant above $\sim$ 6 Å. This short range correlation is quite typical and reflects the fact that the interparticle interaction is also short-ranged. But under the same conditions which create a superfluid energy gap in the present system (thus removing the infrared divergence in the number of excitations), the correlation probability becomes periodic at large distances, representing long range correlations between particles. In this system, because the interparticle interaction and external potential are coherent, they each enhance the other, leading to the highly stable ground state which possesses long-range crystalline order in the density as shown in Fig. 2(a), as well as these long-range particle-particle correlations.

The long-range particle-particle correlations occur *only* when the particles occupy delocalized states and there is an external potential. Because the BT works with the momentum distribution of the quantum field, it does not explicitly give the correlations in the relative motion of the particles [43], but it is likely that these long-range correlations are not fully described by any method which does not explicitly deal with two-body entanglement terms in the many-body wavefunction.

We propose that a more encompassing and physically meaningful measure of superfluidity is the correlation between the motions of particles a sufficiently long distance apart over time scales on the order of the time between perturbations of the system. Since velocity is the derivative of phase, the instantaneous phase correlation described by the first order correlation function is usually a good proxy for short-time velocity correlation. But in this system, the long-range particle-particle correlations that are induced by the external potential result in short time velocity correlation even without strong instantaneous phase correlation.

As described in the Introduction, the advantages of this hybrid system (or one like it [26]) would make strong experimental proof of supersolidity easier to obtain than in currently studied systems because the predicted superfluid fraction is large, even at temperatures above the melting point and lambda point of the bulk. But in addition, an experimental version of this system could provide a controllable testing ground in which we could deepen our understanding of superfluidity and the relative importance of instantaneous phase correlations and short time velocity correlations to produce the interesting macrosopic behavior of superfluid systems.

ACKNOWLEDGMENTS

This work was partially supported by the U.S. Department of Energy Energy Efficiency and Renewable Energy (DOE-EERE) Postdoctoral Research Awards under the EERE Fuel Cell Technologies Program, administered by ORISE for the DOE. ORISE is managed by ORAU (DEAC05-06OR23100). We would like to thank J. Morris, G. Siopsis, and C. Wexler for helpful discussions.

IV. APPENDIX

The solution of a quantum two body-problem with interactions between the two bodies has the general form,

$$\Psi(x_1, x_2) = \psi_1(x_1)\psi_2(x_2)\phi_{12}(x_1 - x_2), \tag{36}$$

where $\phi_{12}(x_1 - x_2)$ represents correlations between the two particles. We assume throughout that the individual terms include the appropriate normalization factors such that an integral of $\Psi^*\Psi$ over all coordinates is equal to one, and define $\rho_1(x_1) = \psi_1^*(x_1)\psi_1(x_1)$, $\rho_{12}(x_1 - x_2) = \phi_{12}^*(x_1 - x_2)\phi_{12}(x_1 - x_2)$ and so forth. Eq. 36 is the solution of the two-body Schrodinger equation,

$$i\hbar\frac{\partial\Psi}{\partial t} = \Big[-\frac{\hbar^2}{2m_1}\nabla_{x_1}^2 - \frac{\hbar^2}{2m_2}\nabla_{x_2}^2 + U(x_1) + U(x_2) + V(x_1 - x_2)\Big]\Psi, \tag{37}$$

where U is the external potential and V is the interaction between the two particles. Because V depends on both position variables, it results in correlations between the two particles in the solution. If $V = 0$, then there are no correlations ($\phi = 1$) and Eq. 37 can be solved exactly by a separation of variables into two independent one-body problems. In other cases, the problem can be simplified by moving to a new coordinate system,

$$X = \frac{m_1x_1 + m_2x_2}{m_1 + m_2}, \tag{38}$$

$$x = x_1 - x_2, \tag{39}$$

$$i\hbar\frac{\partial\Psi}{\partial t} = \Big[-\frac{\hbar^2}{2(m_1 + m_2)}\nabla_X^2 - \frac{\hbar^2 m_1 m_2}{2(m_1 + m_2)}\nabla_x^2 + U\left(X + x\frac{m2}{m1 + m2}\right) + U\left(X - x\frac{m1}{m1 + m2}\right) + V(x)\Big]\Psi. \tag{40}$$

In this new coordinate system, U depends on both position variables, thus the problem can only be solved exactly by separation of variables when $U = 0$.

But often, such as in this work, we are interested in the solution of problems where both U and V are nonzero. A common technique to find an approximate solution to Eq. 37 is mean field theory. The problem is separated into two one-body problems, and the correlation between the two is incorporated by assuming each particle feels only the average effect of the other.

To do this, an ansatz is chosen for the initial form of Ψ. The mean field of the second particle, V_2, is calculated and used to solve the Schrodinger equation for the first particle.

$$V_2(x_1) = \int \rho_2(x_2)\rho_{12}(x_1 - x_2)V(x_1 - x_2)x_2 \tag{41}$$

$$i\hbar\frac{\partial\psi_1}{\partial t} = \left[-\frac{\hbar^2}{2m_1}\nabla_{x_1}^2 + U(x_1) + V_2(x_1)\right]\psi_1, \tag{42}$$

The solutions of ψ_1 are used to calculate the mean field of the first particle $V_1(x_2)$ felt by the second particle, which is then used in the same way to solve the Schrodinger equation for the second particle to find the solutions of solutions of ψ_2. This process can be repeated iteratively until a stable solution is found.

When the particles are identical bosons and we wish to solve for the ground state, the problem becomes even simpler because each particle occupies the same state and thus we only need to solve one set of equations during each iteration to find that state. For N particles using $m_1 = m_2$, the problem becomes

$$V_{N-1}(x_1) = (N-1)\int \rho_1(x_2)\rho_{12}(x_1 - x_2) \times V(x_1 - x_2)dx_2 \tag{43}$$

$$i\hbar\frac{\partial\psi_1}{\partial t} = \left[-\tfrac{\hbar^2}{2m_1}\nabla_{x_1}^2 + U(x_1) + V_{N-1}(x_1)\right]\psi_1, \tag{44}$$

$$\rho_1 = \psi_{1,k=0}^*\psi_{1,k=0}, \tag{45}$$

In most cases, ρ_{12} is assumed to be constant throughout; or rather, some fixed pseudo-potential $V'(x_1 - x_2) \simeq \rho_{12}(x_1 - x_2)V(x_1 - x_2)$ is chosen which approximates ρ_{12} by screening the highly repulsive part of the interaction. However, we could also apply the same mean-field approach to perform a separation of variables on Eq. 40 and find a better solution for ρ_{12}.

$$U_{12}(x) = \int \rho_1(X - x/2)\rho_1(X + x/2) \times [U(X - x/2) + U(X + x/2)]\,dX \tag{46}$$

$$i\hbar\frac{\partial\phi_{12}}{\partial t} = \left[-\frac{\hbar^2}{2m_1}\nabla_x^2 + V(x) + U_{12}(x)\right]\phi_{12}. \tag{47}$$

Since in this work we found a large gap in energy between the ground state and the excited states which change the density of the system, we will assume that we are at some non-zero temperature T which is small enough that the particles all occupy the ground single particle density state (as explained above, there may be phase excitations, but by definition these do not change the density), but large enough that a thermal distribution of ϕ_{12} states are occupied. Thus we estimate the average correlation probability density as,

$$\rho_{12} = \frac{\sum_k e^{E_k/T}\phi_{12,k}^*\phi_{12,k}}{\sum_k e^{-E_k/T}}. \tag{48}$$

This is a zeroth order approximation, which takes into account only thermal depletion of the ground state and not quantum depletion.

Eqs. 43-48 were solved iteratively, starting with ψ equal to the ground state of the single-particle solution of U and $\phi = 1$ as our initial ansatz, and we found that the solution converged quite quickly, with only 3-4 iterations needed. When $U = 0$, as in a bulk system, the lowest energy solution of ϕ_{12} was bound, but only just, with 0.71 K between the bound state and the continuum of unbound states. This is because the ^{4}He-^{4}He potential is weak while the ^{4}He mass is quite small, giving it a relatively

large zero point energy which is comparable to the potential depth, and is the same reason it is difficult to form a bulk solid from ^{4}He. For the set of conditions shown in Figure 6 of the main paper, with $U = -7.87cos(2.06x)$, there was 3.34 K between the bound state and the continuum. But even at $T = 2K$, which was the temperature used for the calculations shown in Figure 6 of the main paper, enough of the unbound states are occupied that ρ_{12} shows long-range correlations between the particles. When the effect of quantum depletion is properly included, there should be long-range correlations even at $T = 0$.

We would also like to emphasize that this long-range correlation occurs only because the particles occupy quantum states which extend over the entire system. At higher temperatures, where the system is more properly described by particles occupying highly localized states, U_{12} will simply be zero because these highly localized states have little overlap, such that $\rho_1(X - x/2)\rho_2(X + x/2) \simeq 0$ for all values of X, x.

[1] A. J. Leggett, Phys. Rev. Lett. **25**, 1543 (1970).
[2] D. Thouless, Ann. Phys. **52**, 403 (1969).
[3] A. Andreev and I. Lifshits, Zh. Eksp. Teor. Fiz. **56**, 2057 (1969).
[4] G. Chester, Phys. Rev. A **2**, 256 (1970).
[5] E. Kim and M. Chan, Nature **427**, 225 (2004).
[6] M. Boninsegni, A. Kuklov, L. Pollet, N. Prokofev, B. Svistunov, and M. Troyer, Phys. Rev. Lett. **97**, 080401 (2006).
[7] A. S. C. Rittner and J. D. Reppy, Phys. Rev. Lett. **97**, 165301 (2006).
[8] A. Clark, J. West, and M. Chan, Phys. Rev. Lett. **99**, 135302 (2007).
[9] D. Y. Kim and M. H. Chan, Phys. Rev. Lett. **109**, 155301 (2012).
[10] M. Boninsegni and N. V. Prokofev, Rev. of Mod. Phys. **84**, 759 (2012).
[11] A. B. Kuklov, N. V. Prokofev, and B. V. Svistunov, Phys. Online J. **4**, 109 (2011).
[12] M. Boninsegni, A. Kuklov, L. Pollet, N. Prokofev, B. Svistunov, and M. Troyer, Phys. Rev. Lett. **99**, 035301 (2007).
[13] P. W. Anderson, Phys. Rev. Lett. **100**, 215301 (2008).
[14] J. Day and J. Beamish, Nature **450**, 853 (2007).
[15] G. Batrouni and R. Scalettar, Phys. Rev. Lett. **84**, 1599 (2000).
[16] F. Hebert, G. G. Batrouni, R. Scalettar, G. Schmid, M. Troyer, and A. Dorneich, Phys. Rev. B **65**, 014513 (2001).
[17] S. Wessel and M. Troyer, Phys. Rev. Lett. **95**, 127205 (2005).
[18] P. Sengupta, L. P. Pryadko, F. Alet, M. Troyer, and G. Schmid, Phys. Rev. Lett. **94**, 207202 (2005).
[19] V. Scarola and S. D. Sarma, Phys. Rev. Lett. **95**, 033003 (2005).
[20] V. Scarola, E. Demler, and S. D. Sarma, Phys. Rev. A **73**, 051601 (2006).
[21] K. Góral, L. Santos, and M. Lewenstein, Phys. Rev. Lett. **88**, 170406 (2002).
[22] M. Anderson, J. Ensher, M. Matthews, C. Wieman, and E. Cornell, Science **269**, 198 (1995).
[23] K. Davis, M. Mewes, M. Andrews, N. Van Druten, D. Durfee, D. Kurn, and W. Ketterle, Phys. Rev. Lett **75**, 3969 (1995).
[24] C. Bradley, C. Sackett, J. Tollett, and R. Hulet, Phys. Rev. Lett **75**, 1687 (1995).
[25] D. Jaksch, C. Bruder, J. I. Cirac, C. W. Gardiner, and P. Zoller, Phys. Rev. Lett. **81**, 3108 (1998).
[26] R. Olsen, Phys. Rev. A, under review; preprint, arXiv:1304.7731.
[27] C. L. Cheung, A. Kurtz, H. Park, and C. M. Lieber, J. Phys. Chem. B **106**, 2429 (2002).
[28] S. Tsang, P. Harris, M. Green, *et al.*, Nature **362**, 520 (1993).
[29] N. N. Bogoliubov, J. Phys. (USSR) **11**, 23 (1947).
[30] L. Pitaevskii and S. Stringari, *Bose-Einstein Condensation* (Oxford University Press, 2003) pp. 30–44.
[31] S. Sunakawa, S. Yamasaki, and T. Kebukawa, Prog. Theor. Phys. **41**, 919 (1969).
[32] J. Javanainen, Phys. Rev. A **54**, 3722 (1996).
[33] G. Quin, W. K, and T. Li, preprint (2001), arXiv:quant-ph/0109020.
[34] A. Solomon, J. of Math. Phys. **12**, 390 (1971).
[35] S. M. Cavaletto and V. Penna, J. Phys. B **44**, 115308 (2011).
[36] J. Morris and R. Gooding, Phys. Rev. B **43**, 6057 (1991).
[37] J. Gottlieb and L. Bruch, Phys. Rev. B **41**, 7195 (1990).
[38] H. J. Lauter, H. Godfrin, and P. Leiderer, J. Low Temp. Phys. **87**, 425 (1992).
[39] T. R. Sosnick, W. M. Snow, P. E. Sokol, and R. N. Silver, Europhys. Lett. **9**, 707 (1989).
[40] P. Hohenberg, Phys. Rev. **158**, 383 (1967).
[41] J. Dupont-Roc, M. Himbert, N. Pavloff, and J. Treiner, J. Low Temp. Phys. **81**, 31 (1990).
[42] V. N. Popov, *Functional integrals in quantum field theory and statistical physics* (Springer, 1987).
[43] A method for calculating particle-particle correlations from parameters of the BT can be found in Lee *et al.* [44], but does not give physical results near the core.
[44] T. D. Lee, K. Huang, and C. N. Yang, Phys. Rev. **106**, 1135 (1957).